ACS APPLIED MATERIALS & INTERFACES

Research Article

www.acsami.org

Luminescent and Transparent Nanopaper Based on Rare-Earth Up-Converting Nanoparticle Grafted Nanofibrillated Cellulose Derived from Garlic Skin

Jingpeng Zhao,[†] Zuwu Wei,[†] Xin Feng,*[,†] Miao Miao,[†] Lining Sun,*[,†] Shaomei Cao,[†] Liyi Shi,[†,‡] and Jianhui Fang[‡]

[†]Research Center of Nano Science and Technology, Shanghai University, Shanghai 200444, P. R. China

[‡]Department of Chemistry, Shanghai University, Shanghai 200093, P. R. China

Supporting Information

ABSTRACT: Highly flexible, transparent, and luminescent nanofibrillated cellulose (NFC) nanopaper with heterogeneous network, functionalized by rare-earth up-converting luminescent nanoparticles (UCNPs), was rapidly synthesized by using a moderate pressure extrusion paper−making process. NFC was successfully prepared from garlic skin using an efficient extraction approach combined with high frequency ultrasonication and high pressure homogenization after removing the noncellulosic components. An efficient epoxidation treatment was carried out to enhance the activity of the UCNPs ($NaYF_4$:Yb,Er) with oleic acid ligand capped on the surface. The UCNPs after epoxidation then reacted with NFC in aqueous medium to form UCNP-grafted NFC nanocomposite (NFC−UCNP) suspensions at ambient temperature. Through the paper-making process, the assembled fluorescent NFC−UCNP hybrid nanopaper exhibits excellent properties, including high transparency, strong up−conversion luminescence, and good flexibility. The obtained hybrid nanopaper was characterized by transmission electron microscopy (TEM), atomic force microscope (AFM), Fourier transform infrared spectroscopy (FTIR), field emission-scanning electron microscope (FE-SEM), up−conversion luminescence (UCL) spectrum, and ultraviolet and visible (UV−vis) spectrophotometer. The experimental results demonstrate that the UCNPs have been successfully grafted to the NFC matrix with heterogeneous network. And the superiorly optical transparent and luminescent properties of the nanopaper mainly depend on the ratio of UCNPs to NFC. Of importance here is that, NFC and UCNPs afford the nanopaper a prospective candidate for multimodal anti-counterfeiting, sensors, and ion probes applications.

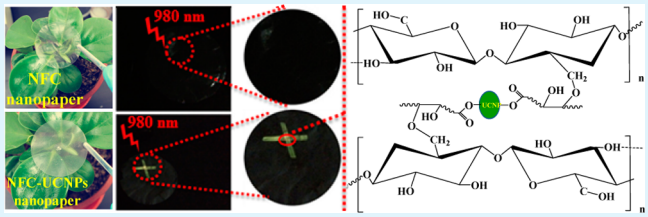

KEYWORDS: *nanofibrillated cellulose, luminescent nanopaper, garlic skin, rare-earth up-converting nanoparticles, extrusion*

INTRODUCTION

Transparent NFC nanopaper with native cellulose nanofibrils as a free-standing skeleton can not only match the desirable ecofriendly sustainability but also introduce new properties such as low thermal expansion, excellent optical and mechanical properties, printability, and enhanced flexibility that can even permit fully folding.[1−5] On the basis of the predominant advantages, the functionalized NFC hybrid nanopaper has received growing interest in the view of exciting characteristics of conductive, fluorescent, and magnetic properties.[6−9] The intriguing application prospects of combining with luminescent materials make it an emerging research area and gather significant attention to security printing, chemical sensors, and heavy metal ion probes.[10−13] For instance, it will act as a lightweight substrate for multilayer covert taggant, bonded with fluorescent dye, to enhance the commercial and forensic security level,[14] and it can also be designed as an alternative for portable oxygen sensor by using UCNPs to photoexcite a quenchable probe for oxygen.[15] Furthermore, the combination of NFC nanopaper and BODIPY-rhodamine is achievable to be developed as a new-fashioned "off−on" ratiometric probe system to selectively detect Hg^{2+} ions on the ppb scale.[16]

To expand the application of cellulose in the optical field, it is advantageous to incorporate some luminescent materials to the cellulose matrices, resulting in the excellently luminescent soft material. Recently, cellulose derivatives incorporated with various fluorescent quantum dots have been paid much attention.[17,18] Several multistep methods are also required to perform fluorescent functionalization of nanofibrillated cellulose (NFC) by incorporation of isothiocyanate,[19−21] succinimidyl ester,[20] and pyrene moieties[22] as fluorescent dopants. However, most of the methods generally concentrate on the modification of cellulose rather than the fluorophores and then give rise to complicated processes to accomplish the labeling, which may result in the complexity of the attachment. Compared to organic fluorophores, rare-earth-doped up−conversion nanoparticles (UCNPs), which undergo an anti-Stokes emission processes

Received: April 30, 2014
Accepted: August 13, 2014
Published: August 13, 2014

Scheme 1. (A) Hierarchical Structure of Garlic Skin Cellulose; (B) Schematic Diagram of Grafting UCNPs on NFC; (C) Pictures of NFC and NFC−UCNP Suspensions; (D) Pictures of NFC and NFC−UCNP Suspensions under Excitation of 980 nm Light with a Power of 2 W; (E) Schematic Diagram of Paper-Making Process; (F) Pictures of NFC Nanopaper and NFC−UCNP Hybrid Nanopaper under Excitation of 980 nm Light with a Power of 2 W

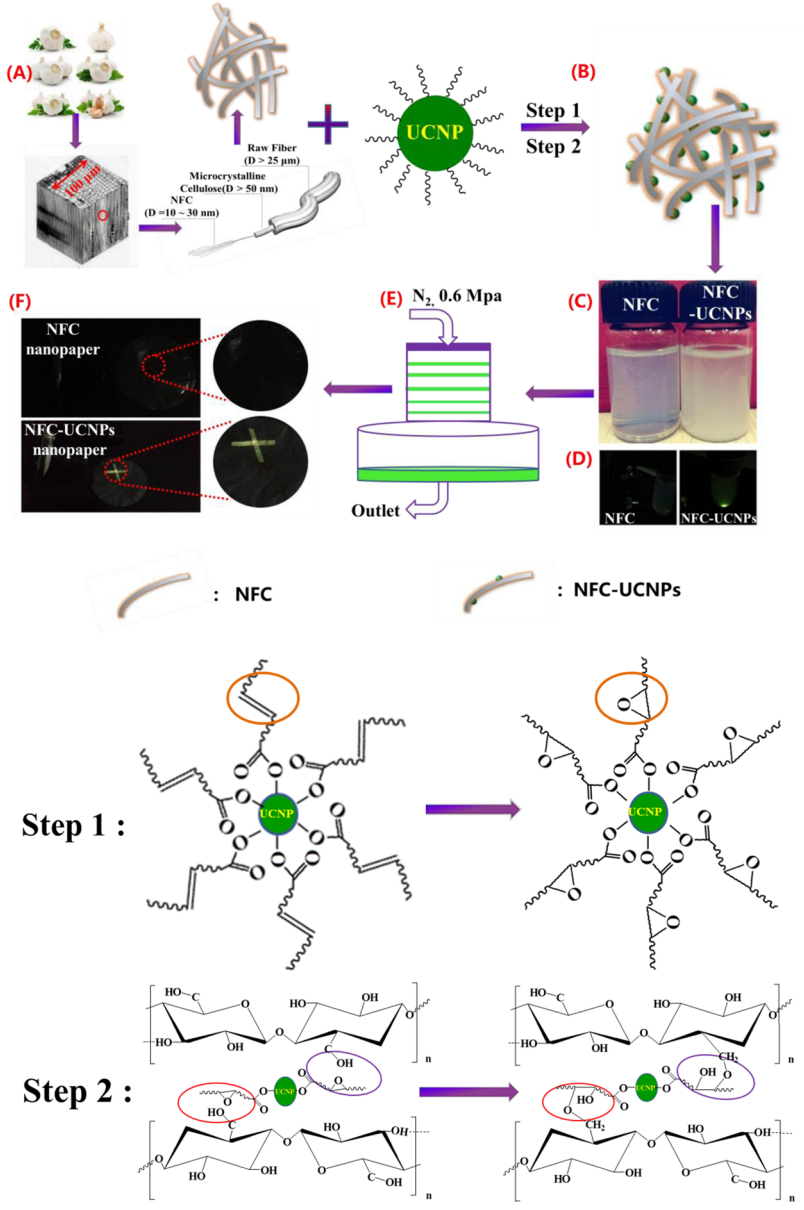

where the long-wavelength pump sources (typically 980 nm) are upconverted to short-wavelength luminescence ranging from the deep-UV to the near-infrared (NIR),[23] have recently drawn much attention in fields as diverse as laser materials, solar cells, data storage and bioapplications.[24,25] To incorporate the UCNPs into the NFC, the challenge is that the UCNPs are difficult to disperse in organic soft matrix because of the unavoidable agglomeration. Therefore, it is necessary and important to modify the UCNPs and control the surface compositions of the NFC.

Usually, the difficulty of making NFC nanopaper is the slow dewatering because of the high water binding capacity of NFC,[17,26] the nanopaper preparation reported in the literature takes from several hours to a few days. Herein, a fast and efficient method for fabrication of NFC nanopaper grafting with UCNPs was designed based on epoxidation of UCNPs and the efficient pressure controlled extrusion paper−making process. The NFC used in this case was successfully isolated from agricultural waste garlic skin, which is economical and frequently left untreated following the harvest season. In the NFC−UCNP nanopaper, the NFC forms the backbone and the UCNPs occupy the spaces and incorporate with NFC to restraint the light scattering that holds transparency and luminescence simultaneously. The luminescent nanopapers with high transparency will offer diversified applications toward the fabrication of new types of NFC-based anti-counterfeiting facilities, sensor systems, and ion probe applications.

EXPERIMENTAL SECTION

Isolation and Preparation of NFC from Garlic Skin. NFC suspension was first prepared from agricultural waste garlic skin in daily life. The procedure was as follows. 10.0 g of garlic skin was pretreated

dx.doi.org/10.1021/am5026352 | ACS Appl. Mater. Interfaces 2014, 6, 14945−14951

and swelled with 2 wt % NaOH aqueous solution (300 g) at 140 °C for 4 h and then filtered with deionized water to remove dissociative pectin and some proteins. The suspension (100 g) after the pectin extracted was ultrasonic smashed with high frequency ultrasonic cell crusher (HighNova instrument Co., Ltd.) at 1000 W for 1 h. The heat−base treated sample was collected and neutralized by vacuum filtration, followed by oven−drying at 70 °C. The residues as-received were heated to 80 °C in the 2 wt % H_2SO_4 aqueous solution (200 g) for 6 h with constant stirring to hydrolyze acid soluble polysaccharides, followed by filtrating and washing to neutral pH. The cellulosic material was bleached at 80 °C for 4 h by 1.5 wt % sodium chlorite (300 g) with pH adjusted to 3−4 by acetic acid. After decoloration, the suspension was centrifuged at 10000 rpm to concentrate the cellulose and eliminate excess liquid until the pH of centrifugation stabilized. Then the cellulose microfibrils separated from garlic skins were subjected to a homogenization process with high pressure homogenizer (D−3L, PhD Technology LLC, USA) for 3 cycles at a pressure level of 172 MPa. Finally, the isolated NFC was obtained by drying process before usage.

Synthesis and Epoxidation of UCNPs. The $NaYF_4$:Yb,Er UCNPs were synthesized according to the literature.[27] In brief, 1.56 mL of YCl_3 (1 M), 0.4 mL of $ErCl_3$ (0.1 M), and 0.4 mL of $YbCl_3$ (1 M) were mixed to a flask and heated to 120 °C to remove water. Second, 30 mL of 1-octadecene and 15 mL of oleic acid were combined with the mixture and heated to 150 °C until a transparent yellow solution appears. Under constant strong stirring at 100 °C, 10 mL of methanol solution containing NH_4F (0.3 g) and NaOH (0.2 g) was introduced, respectively. The synthetic reaction was hold at 300 °C for 1 h in the sand bath under inert atmosphere and then the target UCNPs suspension was obtained. The excess of chemicals were then rinsed out by centrifugation with acetone and cyclohexane. The UCNPs were eventually re−dispersed in 10 mL of cyclohexane and the concentration of the dispersion is 15 mg/mL. The epoxidation modification of fluorescent nanoparticles was achieved by a modified literature procedure.[24] Three mL (15 mg/mL) of as-prepared UCNPs, 1 mL of cyclohexane, 2 mL of dichloromethane, and 5 mg of 3-chloroperoxybenzoic acid were blended in a 100 mL flask consecutively accompanied by condensing equipment, stirred at 40 °C for 2 h. After cooling to room temperature, the re-dispersion in cyclohexane after centrifugation was divided into three parts (volume ratio = 1:2:3) containing 7.5, 15.0, and 22.5 mg of UCNPs , respectively.

Grafting the UCNPs on NFC (NFC−UCNPs). The isometric solution (50 mL) of cyclohexane and dichloromethane (volume ratio = 2:1) including 200 mg of NFC was added into the three containers containing different dosages of modified UCNPs (7.5, 15.0, and 22.5 mg, respectively) and the modified UCNPs was allowed to react with the NFC at room temperature for 10 h under vigorous stirring. The synthesized NFC−UCNPs with different ratio of UCNPs to NFC were eventually re-dispersed in 50 mL of deionized water, respectively.

NFC Mixed with UCNPs without Epoxidation (denoted as NFC(UCNPs)). The as−prepared UCNPs 1.5 mL (22.5 mg) without using 3-chloroperoxybenzoic acid was mixed with NFC by using the same condition with that of NFC−UCNPs. The resultants were centrifuged for 3 times by cyclohexane and 2 times by acetone to remove residual solvent, followed by dialysis by water for 72 h until no fluorescence was detected in the external reservoirs.

Fabrication of Luminescent NFC−UCNP Nanopaper. The extrusion equipment with draining and compression drying units was used to fabricate the hybrid nanopaper based on NFC−UCNP blended suspensions. Five milliliters of the four aqueous NFC−UCNPs suspensions were severally configured to 50 mL with deionized water and ultrasonically dispersed for 20 min. The resultant uniform dispersions were then poured into the extruder (NanoAble-150, PhD Technology LLC, USA), respectively, to squeeze out the excess water within 15 min under 0.6 MPa of N2 gas using a nuclepore track−etch filter membrane (200 nm PC, Whatman, USA). Subsequently, a gel cake emerged on the filter membrane was peeled off and sandwiched between two well-pressed glass plates thoroughly dried at 70 °C. The transparent hybrid nanopapers containing the dosages of UCNPs (0.75, 1.50, and 2.25 mg) with 45 mm in diameter and 40 μm in thickness were ultimately obtained.

The NFC−UCNP nanopaper was soaked in water for 1, 3, 5, and 7 days, respectively, to demonstrate if the UCNPs are firmly bound to the nanopaper.

Characterization. The average particle sizes and morphologies were measured by transmission electron microscopy (TEM) (JEM-2010F, JEOL, Japan) operated at a 120 kV accelerating voltage. DLS measurement of the size distribution of UCNPs was by mean of Zetasizer Nano Z90 (Malvern, UK). Atomic force microscope (AFM) (5500AFM, Agilent, USA) was utilized to tapping mode to image the samples with OMCL-AC160TS standard silicon probes (tip radius <10 nm, spring constant 28.98 N/m, resonant frequency ca. 310 kHz). Fourier transform infrared spectroscopy (FTIR) spectra were recorded in the spectral range from 4000 to 400 cm^{-1} with Thermo Nicolet 6700 spectrometer (Thermo Fisher Scientific, USA) by using pressed KBr tablets. The surface morphologies were observed using a field emission−scanning electron microscope (FE−SEM) (JSM-6700F, JEOL, Japan) at an accelerating voltage of 1.5 kV and a working distance of 6−7 mm. Up−conversion luminescence spectrum (UCL) were recorded on Edinburgh LFS−920 fluorescence spectrometer, with the excitation of an external 2 W semiconductor laser (980 nm, Beijing Hi−tech Optoelectronic Co., China). The up−conversion luminescence photographs were obtained digitally with a Nikon 600D under CW excitation at 980 nm (excitation power 2 W). Light transmittance of the nanopaper was measured using a UV−vis spectrophotometer (2501PC, SHIMADZU, Japan).

RESULTS AND DISCUSSION

The hierarchical structure of garlic skin cellulose and the schematic diagram of NFC nanopaper grafted with UCNPs are shown in Scheme 1. Compared with the multistep methods, the strategy we used is an efficient two-step approach. First, the cyclization reaction of oleic acid ligands with 3-chloroperoxybenzoic acid has been carried out in a mixed solution of cyclohexane and dichloromethane (Scheme 1, Step 1). The epoxide group stemmed from the epoxidation of C═C makes it easy to implement the recombination with −OH in the cellulose (Scheme 1, Step 2). Then the synthesized NFC−UCNPs nanocomposites formed a heterogeneous network as a result of recombination reaction based on the modified UCNPs covalently linking with the NFC (Scheme 1B). The NFC-UCNPs blended suspension appears to be more opaque than the pure NFC suspension (Scheme 1C). The configured NFC−UCNPs suspension was injected into extrusion cylinder controlled by nitrogen pressure (Scheme 1E) to obtain a transparent hybrid nanopaper with highly flexibility. Under the 980 nm laser excitation, no luminescence signal can be observed in both the pure NFC suspension and corresponding NFC nanopaper, however, the green light can be easily detected by the naked eye from the NFC−UCNPs suspension as well as the corresponding NFC−UCNPs nanopaper (Scheme 1D, F). Therefore, it can be deduced that UCNPs were covalently linked with the NFC in the NFC−UCNPs suspension and the corresponding NFC−UCNPs nanopaper.

Generally, the optical transmittance and luminescence properties of the NFC−UCNPs nanopaper are dependent on particle size, and smaller particle size will enhance light transmittance, luminescence, and mechanical performance. However, much smaller particles possess much higher specific surface area and as a result they have a higher tendency to aggregate.[28] Thus, a uniform dispersion of particles with suitable size is significant for optimizing the desired properties of functionalized NFC−UCNPs nanopaper. The TEM image of as-prepared UCNPs shows high monodispersity of the particles approximate 25 nm in diameter and mostly spherical shape (see Figure S1 in the Supporting Information). And the DLS measurement of size

distribution of UCNPs is shown in Figure S2 in the Supporting Information.

Figure 1 shows TEM images of the NFC and NFC−UCNPs. As shown in Figure 1A, the prepared NFC has uniform diameter

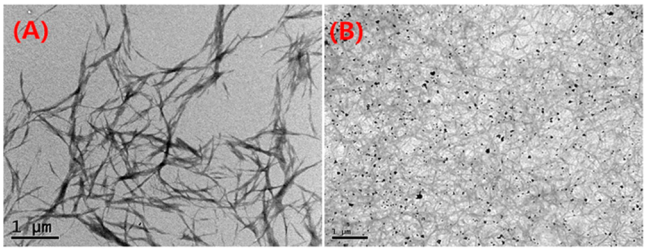

Figure 1. TEM images of (A) NFC and (B) NFC-UCNPs.

distribution and the abundant hydroxyl group contents did not lead to numerous fibers aggregation, which is beneficial to the subsequent paper-making process. The dimension of the NFC is about 20−40 nm in width and 1−3 μm in length, which is necessary for the transparency of nanopaper. In the TEM image of NFC−UCNPs (Figure 1B), the UCNPs were uniformly distributed and combined with NFC closely, similar to the well-dispersed sesame on pizza, suggesting that the modified UCNPs have been well-bonded with NFC.

Figure 2 displays the AFM images and height profiles of the NFC and NFC−UCNPs. It can be noted that the UCNPs have not destroyed the basic structure of the NFC during the grafting process. Images A and D in Figure 2 are the three-dimensional (3D) images of NFC and NFC−UCNPs, respectively. It is quite clear that NFC−UCNPs are thicker than NFC under the same scale. As shown in Figure 2B, the needlelike morphology has been retained well in the NFC, which is in good agreement with the TEM result shown in Figure 1A, but not for the NFC−UCNPs (Figure 2E). The NFC consists mainly of relative smooth nanofibrils, whereas the UCNP-grafted NFC is roller-coated with a layer of accumulated lumps because of bonding UCNPs on the surface of NFC. Moreover, the NFC distribution from the height profile (Figure 2C) indicates that the size distribution is 3−5 nm in height and several micrometers in

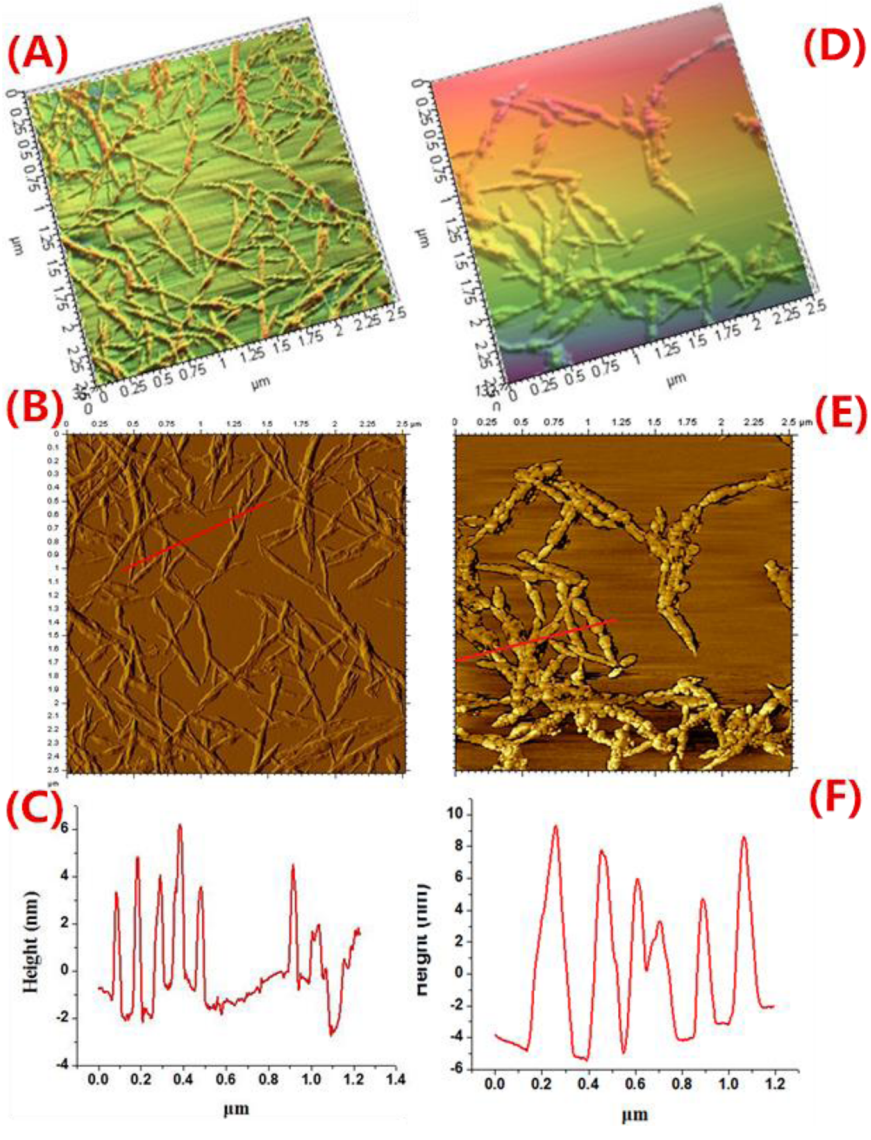

Figure 2. (A−C) NFC and (D−F) NFC-UCNPs: (A, D) 3D AFM images; (B, E) AFM height images; (C, F) height profiles along lines in images of B and E, respectively.

dx.doi.org/10.1021/am5026352 | ACS Appl. Mater. Interfaces 2014, 6, 14945−14951

length, whereas the height of NFC−UCNPs is about 6−10 nm (Figure 2F). From the data of height profiles and visual images, it can be deduced that the UCNPs have been successfully grafted to the superficial layer of the nanofibrils in the NFC-UCNPs. In addition, in comparison with the TEM images (Figure 1), the lateral dimensions from the AFM images are smaller, and the observed dimensional difference may be ascribed to the sample surface concentration on top of the different substrates, i.e., mica for AFM.[29]

The successful attachment of the UCNPs to NFC can also be illustrated by the FTIR spectra. As shown in Figure 3, the

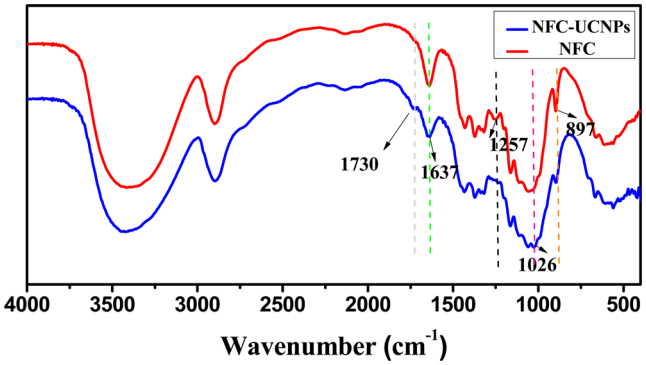

Figure 3. FTIR spectra of the NFC and NFC−UCNPs.

absorption bands at 3418 cm^{-1} is attributed to the stretching vibration of hydroxyl (−OH), and bands at approximately 1430 and 1372 cm^{-1} are assigned to −OCH− in-plane bending and C−H deformation, respectively. The absorption bands at 2898 (C−H stretching), 897 (−COC− deformation), and 657 cm^{-1} (−OH out-of-plane bending) can be observed in the FTIR spectrum of original NFC at the same time,[30] which indicates that the samples derived from garlic skin possess characteristic cellulose functional groups. By contrast, a new peak at 1730 cm^{-1} appeared in the spectrum of the NFC−UCNPs, which was ascribed to the stretching vibration of the group −C═O that originated from the outer layer oleic acid ligand. And both the emergence of a peak at 1026 cm^{-1} corresponding to ν(−COC−) of the composite and the disappear of the infrared absorption peak at 1257 cm^{-1} can prove the labeling reaction between NFC and UCNPs. Meanwhile, the peaks at 1637 (−OH bending) and 897 cm^{-1} in the curve of NFC−UCNPs are much weaker compared with those in NFC, which suggests that the UCNPs have been grafted to the NFC.

SEM images of the surface and fracture section of NFC−UCNPs nanopaper are presented in Figure 4. It can be observed that the network structure of NFC−UCNPs nanopaper is closely

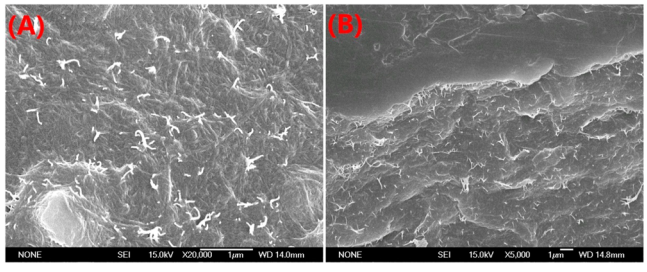

Figure 4. SEM images of the (A) surface and (B) fracture section of NFC−UCNPs nanopaper.

packed after the well-dispersed nanocomposite suspension extruded the excessive solvent and then piled uniformly on the filter membrane. As shown in Figure 4A, the nanofibrils are twined and physically entangled with each other. The predominant orientation appears to be random in the plane. The swirled characteristics are different from the result based on rod−like tunicate whiskers,[31,32] but similar to parenchyma-based cellulose.[33] The length of nanofibril ranges from 2 to 4 μm, and the nanofibril surface profile after grafting UCNPs is not obvious, which may be due to the presence of UCNPs. And more importantly, no excessive difference could be observed in the average width of the fibers. Although the NFC−UCNP nanopaper looks like a thin plastic film by the naked eye, as a matter of fact, it has a unique fibroid structure in the nanoscale that is different from the conventional cellulose paper.[34,35] The fibrillar nature of the material is extremely apparent in the fracture surface as demonstrated in Figure 4B. From Figure 4B, it can be seen that parts of slender nanofibrils from the fracture section of nanopaper were aligned perpendicularly to the breaking direction, indicating that the nanofibrous bundles may be strongly combined together to provide excellent mechanical properties for the NFC−UCNP nanopaper.

Figure 5 shows the UCL spectra of NFC and NFC−UCNPs with UCNPs dosages of 7.5, 15.0, and 22.5 mg, respectively.

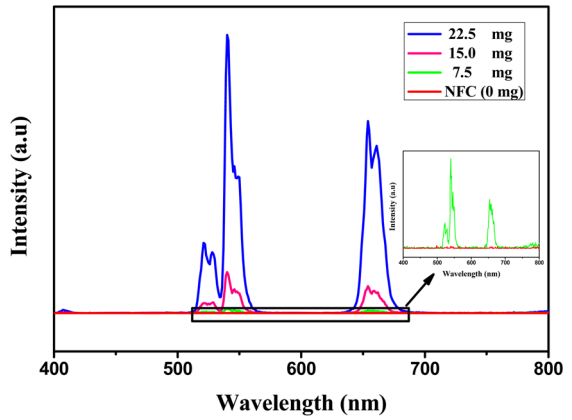

Figure 5. Up−conversion luminescence spectra of NFC (0 mg UCNPs) and NFC−UCNPs with different UCNPs dosages of 7.5, 15, and 22.5 mg, respectively.

Upon excitation with the 980 nm laser, the emission spectra of NFC−UCNPs all exhibited three distinct up−conversion emission bands at 521, 542, and 654 nm, attributed to the $^2H_{11/2} \rightarrow {}^4I_{15/2}$, $^4S_{3/2} \rightarrow {}^4I_{15/2}$, and $^4F_{9/2} \rightarrow {}^4I_{15/2}$ transitions of Er^{3+} ions, respectively,[36,37] and as expected no luminescence was detected for the original NFC. It is also observed that the relative emission intensity of the NFC−UCNP increases when increasing the amount of UCNPs. Then we can infer, in a qualitatively way, that no quenching effects were detected with increasing the amount of UCNPs from 7.5 mg to 22.5 mg, as the experimental conditions (such as excitation power and detection slits) were kept constant during the entire set of measurements. In this case, the pure NFC suspension (containing 0 mg UCNPs) and the same amount (5 mL) of NFC−UCNPs suspensions (containing different doses of UCNPs: 0.75, 1.50, and 2.25 mg, respectively) were used in the following paper−making process.

To demonstrate the epoxidation reaction is necessary to integrate the UCNPs into the NFC, the controlled experiment of NFC mixed with UCNPs without epoxidation was carried out.

The luminescence intensity of NFC(UCNPs) decreased dramatically after the centrifugation and dialysis, while the luminescence intensity of the NFC-UCNPs with epoxidation reaction reserved well (see Figure S3 in the Supporting Information). It can be concluded that the UCNPs are firmly bonded to the NFC in the NFC-UCNPs, but not in the NFC(UCNPs). To further confirm the UCNPs are firmly bonded to the nanopaper sheet, the NFC-UCNPs nanopaper was soaked in water for different time, 1, 3, 5, and 7 days, respectively. The luminescence intensities seem to be unchanged by the naked eyes, as shown in Figure S4 in the Supporting Information. To illustrate that the whole nanopaper has the homogeneous up−converision luminescence, we made a dynamic movie in the case of mobile under the 980 nm laser excitation (see the video in the Supporting Information).

The relationship between the transparency and the doping amount of UCNPs in the NFC-UCNPs nanopaper was investigated (see Figure 6). Figure 6A−C displays the NFC−

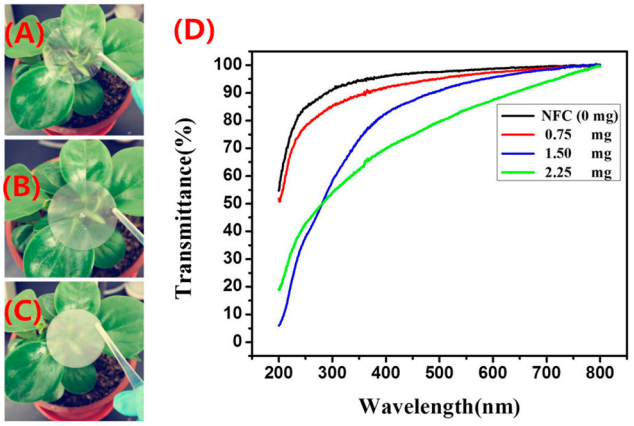

Figure 6. Pictures of NFC−UCNPs hybrid nanopapers with different UCNPs dosages of (A) 0.75 mg, (B) 1.50 mg, and (C) 2.25 mg; (D) transmittance curves for nanopapers with different UCNPs dosages.

UCNPs nanopapers with different UCNPs dosages of 0.75 mg, 1.50 mg, 2.25 mg, respectively. It is obvious that the transmittance of nanopaper can be tuned by the content of UCNPs immobilized into the NFC network. With the increased stoichiometric ratio of UCNPs to NFC in the nanopaper, the green plant under the nanopaper is more obscure, that is to say, the NFC nanopaper grafted with more UCNPs, the lower transmittance. It is precisely because that the UCNPs are uniformly grafted on the NFC to strengthen the fibrils, which results in the increase in light scattering and decrease in transparency. Reducing the diameter of cellulose fibers will decrease the optical scattering and improve the transparency of NFC nanopapers.[38] The nanopaper composed of nanofibrils with the diameters of ~10 nm can possess a high transmittance of more than 90% at wavelength of larger than 550 nm[39] and a 3D fiber network structure with high flexibility.[40] For the NFC−UCNP hybrid nanopapers in our case, at wavelength of larger than 550 nm, even the proportion of UCNPs comes to its maximum 2.25 mg, for the nanopaper 83% transmittance can be still reachable, while for the nanopaper with 0.75 mg UCNPs 96% highest transmittance can be obtained (Figure 6D). Therefore, they are good enough to have potential applications for optoelectronic devices such as thin nanopaper solar cells since the efficiency of a thin nanopaper solar cell will be influenced by the light trapping. Furthermore, serving as an outdoor electronic display such as touch screen displays may be a still further sensible pathway.[41] Taking the economic effects into account, the NFC nanopaper depends on time-saving manufacturing method and plentifully raw resources of cellulose, which would render it cheaper and practically feasible.

CONCLUSION

To the best of our knowledge, this is the first up−conversion luminescent NFC nanopaper, consisting of NFC from garlic skin as the backbone and the UCNPs as additives for elongating the fibrous network. The UCNPs has grafted to the NFC successfully, and resulting in the up−conversion luminescent thin nanopaper upon 980 nm excitation. And the luminescent intensity and transmittance of the nanopaper can be controlled by changing the amount of UCNPs. The method of grafting UCNPs to NFC provides an extended and general approach to be available for other multifunctional luminescent materials. The obtained NFC-UCNPs nanopaper exhibits many predominant advantages, including uniformity, close-grained property, low cost, and up−conversion luminescence. Such superiorly luminescent NFC nanopaper with high optical transmittance controlled by the tagging content of the UCNPs will widely arouse tremendous interests in the industry.

ASSOCIATED CONTENT

Supporting Information

TEM image of UCNPs in Figure S1; DLS measurement of the size distribution of UCNPs in Figure S2; up−conversion luminescence spectra of NFC-UCNPs and NFC(UCNPs) in Figure S3; pictures of NFC-UCNPs nanopaper in bright field and in dark field under excitation of 980 nm light in Figure S4; video (AVI). This material is available free of charge via the Internet at http://pubs.acs.org/.

AUTHOR INFORMATION

Corresponding Authors

*E-mail: fengxin@shu.edu.cn.
*E-mail: lnsun@shu.edu.cn.

Notes

The authors declare no competing financial interest.

ACKNOWLEDGMENTS

This work was financially supported by the Science and Technology Commission of Shanghai Municipality (13ZR1415100, 13JC1402700, 13NM1401101, 13DZ2292100), the National Natural Science Foundation of China (Grants 21001072, 21231004), Innovation Program of Shanghai Municipal Education Commission (13ZZ073), Shanghai Foundation of Excellent Young University Teacher, and Shanghai Rising-Star Program (14QA1401800). We are also grateful to Instrumental Analysis & Research Center of Shanghai University.

REFERENCES

(1) Henriksson, M.; Berglund, L. A.; Isaksson, P.; Nishino, T.; Lindstrom, T. Cellulose Nanopaper Structures of High Toughness. *Biomacromolecules* **2008**, *9*, 1579−1585.
(2) Nogi, M.; Iwamoto, S.; Nakagaito, A. N.; Yano, H. Optically Transparent Nanofiber Paper. *Adv. Mater.* **2009**, *21*, 1595−1598.
(3) Russo, A.; Ahn, B. Y.; Adams, J. J.; Duoss, E. B.; Bernhard, J. T.; Lewis, J. A. Pen-on-Paper Flexible Electronics. *Adv. Mater.* **2011**, *23*, 3426−3430.

(4) Sehaqui, H.; Zhou, Q.; Ikkala, O.; Berglund, L. A. Strong and Tough Cellulose Nanopaper with High Specific Surface Area and Porosity. *Biomacromolecules* **2011**, *12*, 3638−3644.
(5) Bollström, R.; Määttänen, A.; Tobjörk, D.; Ihalainen, P.; Kaihovirta, N.; Österbacka, R.; Peltonen, J.; Toivakka, M. A Multilayer Coated Fiber−based Substrate Suitable for Printed Functionality. *Org. Electron.* **2009**, *10*, 1020−1023.
(6) Hu, L.; Wu, H.; Mantia, F. L.; Yang, Y.; Cui, Y. Thin, Flexible Secondary Li−Ion Paper Batteries. *ACS Nano* **2010**, *4*, 5843−5848.
(7) Li, Y.; Zhu, H.; Gu, H.; Dai, H.; Fang, Z.; Weadock, N. J.; Guo, Z.; Hu, L. Strong Transparent Magnetic Nanopaper Prepared by Immobilization of Fe_3O_4 Nanoparticles in Nanofibrillated Cellulose Network. *J. Mater. Chem. C* **2013**, *1*, 15278−15283.
(8) Yan, D.; Williams, G. R.; Zhao, M.; Li, C.; Fan, G.; Yang, H. Flexible Free−standing Luminescent Two-component Fiber Nanopapers with Tunable Hierarchical Structures Based on Hydrogen−Bonding Architecture. *Langmuir* **2013**, *29*, 15673−15681.
(9) Olsson, R. T.; Azizi Samir, M. A. S.; Salazar-Alvarez, G.; Belova, L.; Ström, V.; Berglund, L. A.; Ikkala, O.; Nogués, J.; Gedde, U. W. Making Flexible Magnetic Aerogels and Stiff Magnetic Nanopaper Using Cellulose Nanofibrils as Templates. *Nat. Nanotechnol.* **2010**, *5*, 584−588.
(10) Christian, S. E.; Liam, R. B.; Stephen, M.; John, D. G.; Daniel, R. G.; Patrick, D. L. Zero−reabsorption Doped−Nanocrystal Luminescent Solar Concentrators. *ACS Nano* **2014**, *8*, 3461−3467.
(11) Song, L.; Jiao, C.; David, T. P.; Zhao, J. X. A Turn−on Fluorescent Nanoprobe for Selective Determination of Selenium (IV). *ACS Appl. Mater. Interfaces* **2013**, *5*, 5165−5173.
(12) Wang, L.; Li, Y. Controlled Synthesis and Luminescence of Lanthanide Doped $NaYF_4$ Nanocrystals. *Chem. Mater.* **2007**, *19*, 727−734.
(13) Zheng, M.; Xie, Z.; Qu, D.; Li, D.; Du, P.; Jing, X.; Sun, Z. On−Off−On Fluorescent Carbon Dot Nanosensor for Recognition of Chromium (VI) and Ascorbic Acid Based on the Inner Filter Effect. *ACS Appl. Mater. Interfaces* **2013**, *5*, 13242−13427.
(14) Binh, D.; Liu, H.; Li, C.; Deng, W.; Ma, L. Printed Multilayer Microtaggants with Phase Change Nanoparticles for Enhanced Labeling Security. *ACS Appl. Mater. Interfaces* **2014**, *6*, 8909−8912.
(15) Achatz, D.; Meier, R. J.; Fischer, L. H.; Wolfbeis, O. S. Luminescent Sensing of Oxygen Using a Quenchable Probe and Upconverting Nanoparticles. *Angew. Chem., Int. Ed.* **2011**, *50*, 260−263.
(16) Zhang, X.; Xiao, Y.; Qian, X. A Ratiometric Fluorescent Probe Based on FRET for Imaging Hg^{2+} Ions in Living Cells. *Angew. Chem., Int. Ed.* **2008**, *47*, 8025−8029.
(17) Junka, K.; Guo, J.; Filpponen, I.; Laine, J.; Rojas, O. J. Modification of Cellulose Nanofibrils with Luminescent Carbon Dots. *Biomacromolecules* **2014**, *15*, 876−881.
(18) Chang, C.; Peng, J.; Zhang, L.; Pang, D. W. Strongly Fluorescent Hydrogels with Quantum Dots Embedded in Cellulose Matrices. *J. Mater. Chem.* **2009**, *19*, 7771−7776.
(19) Dong, S.; Roman, M. Fluorescently Labeled Cellulose Nanocrystals for Bioimaging Applications. *J. Am. Chem. Soc.* **2007**, *129*, 13810−13811.
(20) Eyley, S.; Thielemans, W. Imidazolium Grafted Cellulose Nanocrystals for Ion Exchange Applications. *Chem. Commun.* **2011**, *47*, 4177−4179.
(21) Mahmoud, K. A.; Mena, J. A.; Male, K. B.; Hrapovic, S.; Kamen, A.; Luong, J. H. Effect of Surface Charge on the Cellular Uptake and Cytotoxicity of Fluorescent Labeled Cellulose Nanocrystals. *ACS Appl. Mater. Interfaces* **2010**, *2*, 2924−2932.
(22) Zhang, L.; Li, Q.; Zhou, J.; Zhang, L. Synthesis and Photophysical Behavior of Pyrene−Bearing Cellulose Nanocrystals for Fe^{3+} Sensing. *Macromol. Chem. Phys.* **2012**, *213*, 1612−1617.
(23) Sun, L.; Qiu, Y.; Liu, T.; Zhang, J. Z.; Dang, S.; Feng, J.; Wang, Z.; Zhang, H.; Shi, L. Near Infrared and Visible Luminescence from Xerogels Covalently Grafted with Lanthanide [Sm^{3+}, Yb^{3+}, Nd^{3+}, Er^{3+}, Pr^{3+}, Ho^{3+}] β-Diketonate Derivatives Using Visible Light Excitation. *ACS Appl. Mater. Interfaces* **2013**, *5*, 9585−9593.
(24) Wei, Z.; Sun, L.; Liu, J.; Zhang, J. Z.; Yang, H.; Yang, Y.; Shi, L. Cysteine Modified Rare-earth Up−converting Nanoparticles for in Vitro and in Vivo Bioimaging. *Biomaterials* **2014**, *35*, 387−392.
(25) Liu, Z.; Sun, L.; Li, F.; Liu, Q.; Shi, L.; Zhang, D.; Yuan, S.; Liu, T.; Qiu, Y. One-pot Self−assembly of Multifunctional Mesoporous Nanoprobes with Magnetic Nanoparticles and Hydrophobic Upconversion Nanocrystals. *J. Mater. Chem.* **2011**, *21*, 17615−17618.
(26) Österberg, M.; Vartiainen, J.; Lucenius, J.; Hippi, U.; Seppälä, J.; Serimaa, R.; Laine, J. A Fast Method to Produce Strong NFC Nanopapers as a Platform for Barrier and Functional Materials. *ACS Appl. Mater. Interfaces* **2013**, *5*, 4640−4647.
(27) Li, Z.; Zhang, Y.; Jiang, S. Multicolor Core/Shell−Structured Upconversion Fluorescent Nanoparticles. *Adv. Mater.* **2008**, *20*, 4765−4769.
(28) Barnakov, Y. A.; Scott, B. L.; Golub, V.; Kelly, L.; Reddy, V.; Stokes, K. L. Spectral Dependence of Faraday Rotation in Magnetite−polymer Nanocomposites. *J. Phys. Chem. Solids* **2004**, *65*, 1005−1010.
(29) Lacava, L. M.; Lacava, B. M.; Azevedo, R. B.; Lacava, Z. G. M.; Buske, N.; Tronconi, A. L.; Morais, P. C. Nanoparticle Sizing: A Comparative Study Using Atomic Force Microscopy, Transmission Electron Microscopy, and Ferromagnetic Resonance. *J. Magn. Magn. Mater.* **2011**, *225*, 79−83.
(30) Oh, S. Y.; Yoo, D. I.; Shin, Y.; Seo, G. FTIR Analysis of Cellulose Treated with Sodium Hydroxide and Carbon Dioxide. *Carbohydr. Res.* **2005**, *340*, 417−428.
(31) Favier, V.; Canova, G. R.; Cavaille, J. Y.; Chanzy, H.; Dufresne, A.; Gauthier, C. Nanocomposite Materials from Latex and Cellulose Whiskers. Polym. *Adv. Technol.* **1995**, *6*, 351−355.
(32) Favier, V.; Chanzy, H.; Cavaille, J. Y. Polymer Nanocomposites Reinforced by Cellulose Whiskers. *Macromolecules* **1995**, *28*, 6365−6367.
(33) Samir, M. A. S. A.; Alloin, F.; Paillet, M.; Dufresne, A. Tangling Effect in Fibrillated Cellulose Reinforced Nanocomposites. *Macromolecules* **2004**, *37*, 4313−4316.
(34) Henriksson, M.; Fogelström, L.; Berglund, L. A.; Johansson, M.; Hult, A. Novel Nanocomposite Concept Based on Cross−linking of Hyperbranched Polymers in Reactive Cellulose Nanopaper Templates. *Compos. Sci. Technol.* **2011**, *71*, 13−17.
(35) Moon, R. J.; Martini, A.; Nairn, J.; Simonsen, J.; Youngblood, J. Cellulose Nanomaterials Review: Structure, Properties and Nanocomposites. *J. Chem. Soc. Rev.* **2011**, *40*, 3941−3994.
(36) Liu, Q.; Chen, M.; Sun, Y.; Chen, G.; Yang, T.; Gao, Y.; Zhang, X.; Li, F. Multifunctional Rare-earth Self-assembled Nanosystem for Tri−modal Upconversion Luminescence/Fluorescence/Positron Emission Tomography Imaging. *Biomaterials* **2011**, *32*, 8243−8253.
(37) Cao, T.; Yang, Y.; Sun, Y.; Wu, Y.; Gao, Y.; Feng, W.; Li, F. Hydrothermal Synthesis of $NaLuF_4$:^{153}Sm,Yb,Tm Nanoparticles and Their Application in Dual-modality Upconversion Luminescence and SPECT Bioimaging. *Biomaterials* **2013**, *34*, 7127−7134.
(38) Zhu, H.; Fang, Z.; Preston, C.; Li, Y.; Hu, L. Transparent Paper: Fabrications, Properties, and Device Applications. *Energy Environ. Sci.* **2014**, *7*, 269−313.
(39) Zhu, H.; Parvinian, S.; Preston, C.; Vaaland, O.; Ruan, Z.; Hu, L. Transparent Nanopaper with Tailored Optical Properties. *Nanoscale* **2013**, *5*, 3787−3792.
(40) Zhang, W.; Zhang, X.; Lu, C.; Wang, Y.; Deng, Y. Flexible and Transparent Paper−Based Ionic Diode Fabricated from Oppositely Charged Microfibrillated Cellulose. *J. Phys. Chem. C* **2012**, *116*, 9227−9234.
(41) Fang, Z.; Zhu, H.; Preston, C.; Han, X.; Li, Y.; Lee, S.; Chai, X.; Chen, G.; Hu, L. Highly Transparent and Writable Wood All-cellulose Hybrid Nanostructured Paper. *J. Mater. Chem. C* **2013**, *1*, 6191−6197.